



# CHORUS

This is the accepted manuscript made available via CHORUS. The article has been published as:

## Detecting deterministic nature of pressure measurements from a turbulent combustor

J. Tony, E. A. Gopalakrishnan, E. Sreelekha, and R. I. Sujith

Phys. Rev. E **92**, 062902 — Published 2 December 2015

DOI: [10.1103/PhysRevE.92.062902](https://doi.org/10.1103/PhysRevE.92.062902)

# Detecting deterministic nature of pressure measurements from a turbulent combustor

Tony J.\* and Gopalakrishnan, E. A., Sreelekha, E. and Sujith, R. I.  
*Department of Aerospace Engineering, IIT Madras, Chennai, India*

Identifying nonlinear structures in a time series, acquired from real world systems, is essential to characterize the dynamics of the system under study. A single time series alone might be available in most experimental situations. In addition to this, conventional techniques such as power spectral analysis might not be sufficient to characterize a time series if it is acquired from a complex system such as a thermo-acoustic system. In this study, we analyze the unsteady pressure signal acquired from a turbulent combustor with bluff-body and swirler as flame holding devices. The fractal features in the unsteady pressure signal are identified using the singularity spectrum. Further, we employ surrogate methods, with translational error and permutation entropy as discriminating statistics, to test for determinism visible in the observed time series. In addition to this, permutation spectrum test could prove to be a robust technique to characterize the dynamical nature of the pressure time series acquired from experiments. Further, measures such as correlation dimension and correlation entropy are adopted to qualitatively detect noise contamination in the pressure measurements acquired during the state of combustion noise. These ensemble of measures is necessary to identify the features of a time series acquired from a system as complex as a turbulent combustor. Using these measures, we show that the pressure fluctuations during combustion noise has the features of a high dimensional chaotic data contaminated with white and colored noise.

## I. INTRODUCTION

Thermo-acoustic instability is a dynamic phenomenon marked by the presence of large amplitude, self-excited pressure oscillations established in a confinement as a result of complex combustion acoustic interactions [1–3]. Such oscillations often lead to the failure of combustion systems due to excessive vibration of the hardware [4] and increased heat transfer to the walls of the chamber [5]. In many turbulent combustion systems, these thermo-acoustic oscillations are preceded by an intermittent regime. Further, prior to intermittency, there exists a state that is dictated by low amplitude aperiodic fluctuations in pressure and velocity measurements. The transition of the system from this stable state, the so called combustion noise, to thermo-acoustic instability, has become the focus of studies on combustion dynamics in recent years [6–13].

There have been successful attempts to predict the transition to instability that is observed in a thermo-acoustic system. Certain features inherent to combustion noise were identified in order to devise predictive measures such as Hurst exponent and translational error [9, 11]. These measures are sensitive to the changes in the system dynamics during the transition from aperiodic to periodic pressure oscillations. However, understanding this transition would require identifying the deterministic or stochastic nature of these aperiodic pressure fluctuations acquired during the state of combustion noise. Understanding the nature of combustion noise is important, so as to model and study the transition in detail. It is worth emphasizing that these transitions are observed

not just in thermo-acoustic systems, but also in aeroelastic [14, 15] and aeroacoustic systems [16]. Therefore, understanding the physics of this transition will be of interest to a wide range of fields. In order to accomplish this, the dynamics of the base state of the system must be clearly understood. Further, models developed to describe these transitions must capture the features of the base state accurately.

In literature, a stochastic description is generally adopted to model the sources of combustion noise [17]. In the traditional approach, the effects of turbulence are often modelled using additive noise sources, while analyzing thermo-acoustic instability [18, 19]. Any approach to understand the combustion dynamics basically reduces the problem to an acoustic problem, once the description of hydrodynamic processes is bypassed. The relevance of such analyses, where the effects of turbulence are modeled using stochastic sources, depends on the problem at hand. Moreover, it might be insufficient to capture the dynamics of combustion noise, if it occurs that the pressure measurements indeed have a deterministic signature.

Recent studies indicate that the pressure measurements acquired during the stable operation in turbulent combustors display multifractal features [11] and its dynamics has been attributed to deterministic chaos [8]. In these studies, measures such as Kaplan-Glass test and 0-1 test along with randomly shuffled surrogate test were employed to identify the dynamic nature of combustion noise. A simple surrogate test such as random shuffling, that eliminates temporal correlations in the signal, does not provide conclusive proof for determinism in the time series. However, the fact that those studies were focused on devising appropriate precursors to instability must be acknowledged.

Gotoda *et al.* (2011), in an attempt to identify the nature of pressure fluctuations near lean blowout in a

---

\* Corresponding author.  
Email: tonyjohnny1994@gmail.com

lean-premixed combustor, adopted methods of nonlinear time series analysis to interpret such fluctuations from a stochastic viewpoint. They illustrated the need to adopt sophisticated nonlinear techniques to extract the degree of determinism visible in the observed time series. Further, they observed the transition of the system from stochastic fluctuations to periodic oscillations through low dimensional chaos, with increases in equivalence ratio. Translational error was used as a measure to characterize the observed time series as stochastic and chaotic in different parameter regimes. It must be noted that, they employed appropriate surrogate tests to support this analysis. In a subsequent paper, Gotoda *et al.* (2012) adopted the permutation entropy in combination with surrogate data methods to discuss the possible existence of chaotic fluctuations in the pressure measurements. In short, it is clear from earlier studies that identifying the dynamic nature of an experimental time series is not trivially obvious.

A basic understanding of the physical processes involved in the dynamic behavior of the system is sufficient to choose appropriate tools for analyzing the acquired time series. Power spectral methods, that detect linear correlations in the signal, are often insufficient to capture the intricacies of the measured time series. The framework of nonlinear dynamics, inspired from the recent advances in the field, well serves the purpose of this analysis. A thermoacoustic system can be viewed as a complex dynamical system owing to the nonlinear processes and time lags involved in the temporal evolution of the system. The presence of time delays in the physical system makes it a high dimensional dynamical system [20]. Recent studies on thermoacoustic phenomenon from the viewpoint of nonlinear dynamics reveal the existence of different dynamical states such as chaos [8, 21], intermittent bursts [9, 10, 22], quasiperiodic oscillations [22] and so on.

In principle, to represent a complex system, all the state variables that govern the evolution of the system must be known. However, in an experimental situation, only a subset of these variables can actually be measured. Moreover, the objective in practical situations is to identify the processes involved in the dynamics of the system from the available data sets, which falls under the category of an inverse problem [23]. The first step towards identifying the underlying process is to correctly characterize the time series that is generated out of it. In this analysis, a scalar time series, the acoustic pressure  $p'(t)$  is often the only data available from experiments. The time series of unsteady pressure acquired during combustion noise appear noisy. However, the temporal correlations identified in the measured signal necessarily mean that the data cannot be disregarded as mere random fluctuations [11]. These fluctuations can be due to the influence of pseudo periodic elements, chaos, linear or nonlinear correlations, dynamic or observational noise [23]. However, it is difficult to identify the nature of an experimental time series as it is highly likely to be contaminated

with noise. The difficulty is more pronounced when the time series measurements are acquired from a complex system such as a thermoacoustic system [24]. There can be cases where an experimental time series is contaminated by dynamic as well as observational noises. Taking into account of such complexities, a conclusive approach must be adopted to accurately determine the dynamic nature of the pressure measurements. A complete analysis to recognize the dynamic nature of these aperiodic fluctuations could aid the studies on transitions to another stable state.

In this study, the time series is analyzed under the assumption that it is generated out of either stochastic or purely deterministic dynamics. Tests that can detect nonlinearity and fractal features in a signal must be performed to conclusively diagnose chaotic elements, if present, in the time series [25]. Measures such as generalized Hurst exponents and singularity spectrum are used to identify the scaling behavior of the pressure signal obtained from experiments. However, the presence of fractal features, though necessary, is not sufficient to conclude that the observed time series is chaotic. This is because; correlated noise might as well possess scaling behavior similar to that of a chaotic signal [26]. Therefore, measures that can detect nonlinearity in a time series must be adopted, in addition to fractal measures, for quantifying deterministic chaos that is manifested in the time series. Direct tests, such as Lyapunov exponent and correlation dimension, are normally adopted to claim the evidence of chaos in a time series. A sensitive dependence on initial conditions is the standard basis to detect the chaotic nature in deterministic dynamical systems [27]. Lyapunov exponent is a measure that quantifies the exponential divergence of nearby trajectories of an attractor in the state space. A system with one or more positive Lyapunov exponents is defined to be chaotic. Oseledec theorem [28], applicable to continuous and differentiable equations, is used to develop algorithms for calculating Lyapunov exponents [29]. However, this approach may not work for experimental data contaminated with noise and the qualitative behavior of such a signal is not merely dictated by the sign of Lyapunov exponents [27, 29].

Standard methods such as Grassberger-Procaccia (GP) algorithm, used to find correlation dimension, can recognize chaotic time series; however, the procedure requires the identification of the scaling region in the correlation sum by visual inspection, in order to correctly estimate the dimension [30]. In practical data contaminated with dynamic or observational noise, identifying the appropriate scaling region in phase space becomes more difficult [30]. In the case of a short time series, the value for correlation dimension obtained using the GP algorithm might not be the actual dimension of the attractor. It would rather be the result of using a short time series for the analysis [31]. The inherent limitations posed by these techniques will be exposed while analyzing noisy data.

Direct tests are therefore, not sufficient to claim evi-

dence of determinism in a time series acquired from experiments [32]. The other alternative, surrogate tests, is merely an extension of direct tests; however, it is basically a statistical test. A null hypothesis  $q$  is formulated for a given data set and its validity is examined through this statistical test [23]. A null hypothesis is basically a claim made on the origin of the data sets under analysis. First, we generate surrogate data sets consistent with the null hypothesis that one has to test for. Then, we compute a suitable nonlinear statistic, also known as discriminating statistic ( $T$ ), for the original data set and for the ensemble of surrogate data sets [23]. If the computed values of statistic for the original data and set of surrogates are significantly different, one can safely argue that the data were not generated by a process described by the null hypothesis. However, the null hypothesis cannot be falsified with absolute certainty. Instead, rejection is carried out in a probabilistic sense; i.e., at a certain confidence level, determined by the number of surrogate data sets, generated according to any particular hypothesis [23]. The distribution of the statistic,  $T$  (for the surrogate data sets) obtained according to the the null hypothesis, can be estimated. Then, the rejection region is chosen at the tail of the distribution based on a given significance level  $t$  [33]. The significance level  $t$  is given by,

$$t = \frac{|T - \langle T \rangle_{surr}|}{\sigma_{surr}} \quad (1)$$

where  $T$  is the statistic,  $\langle T \rangle_{surr}$  is the mean of the statistic evaluated for the surrogate data sets and  $\sigma_{surr}$  is the standard deviation for the surrogates [30]. In short, surrogate tests are necessary to assess the confidence level associated with any of the estimates for the metrics adopted. The most commonly used techniques to generate surrogate data for statistical analysis of nonlinear processes include random shuffling of original series, Fourier transformed (FT) surrogates and amplitude adjusted Fourier transformed (AAFT) surrogates.

Random shuffling or random permutation (RP) is the simplest way of generating surrogate data [23]. The elements of the original data set are randomly rearranged so as to destroy any linear correlations present, if any, in the data while preserving its distribution. This method is consistent with the null hypothesis that the data is generated from an uncorrelated random process. Rejection of this hypothesis means that the signal possesses temporal correlations. Testing the time series against this hypothesis must be a trivial exercise in most cases as the time series data obtained from experiments might possess temporal correlations. To deal with correlated time series data, an algorithm was developed by Theiler *et al.* (1992) for testing the null hypothesis of a linear stochastic process [34]. Rejection of this hypothesis necessarily means that the data being tested do not stem from a linear Gaussian process. To implement this surrogate test, the mean and covariance of the surrogate data sets should match with that of the original data. In practice, the algorithms for FT surrogate maintains the

amplitude spectrum of the time series while randomizing the Fourier phases [34]. The underlying phase can be chosen randomly from a uniform distribution on  $[0, 2\pi]$ . This is because; the Fourier phases of a linear Gaussian process do not contain any useful information, as the features of such a process can be completely determined by their mean and autocovariance function [33]. Further, it is known by the Wiener-Khinchin theorem, that the autocovariance function has a one to one correspondence with the power spectrum via the Fourier transformation [35].

In practical cases, the time series acquired from experiments might be contaminated with observational noise as well as dynamic noise. The probability distribution of the data originating from a linear Gaussian process might deviate from a normal distribution if the data is contaminated with observational noise. Thus, the nonlinearity in the signal might be an artifact of the measurement system. The AAFT surrogate test was hence developed so as to resolve the limitations that arise when the original data do not follow a Gaussian probability distribution [36]. This test is based on the null hypothesis that the original data is derived from a linear Gaussian process, modified by a nonlinear measurement function [34]. The steps involved in generating an AAFT surrogate data set are as follows. Consider  $x_n$ ,  $n = 1, 2, \dots, N$  to be the observed time series. According to the null hypothesis,  $x_n = h(s_n)$ , where  $s_n$  is a realization of a linear Gaussian process and  $h$  is a nonlinear measurement function. Methods that implement AAFT try to invert the measurement function by changing the distribution of the original data to obtain a Gaussian distribution [33]. This is performed by assigning a rank to the elements in the time series by comparing the relative values of the elements. A white noise data (Gaussian) of the same length as the original data is rearranged to obtain the same rank structure as the original time series. A phase randomized surrogate of the rearranged data (Gaussian) is then constructed. Further, the transformed data is reordered in such a way that the original data and the resultant surrogate have the same rank order [34]. The results from this test turn out to be accurate, when the number of data points in the signal is large and the measurement function is almost an identity function [33]. Rejection of the null hypothesis of AAFT, FT and random shuffle is an indication of the presence of nonlinearity in the measured signal.

The successful application of statistical hypothesis testing relies on the choice of the discriminating statistic. The statistics used in this study require reconstructing the phase space from the measured time series data using Takens' embedding theorem. Techniques are available to estimate the optimum delay ( $\tau$ ) and embedding dimension ( $D$ ), which are necessary to accurately reconstruct the state space [37]. Through delay embedding, the scalar time series is converted into a set of delayed vectors, which helps in visualizing the system dynamics at different conditions. An important statistic that can

possibly distinguish the original data from the surrogate data sets will be the translational error, if the time series under analysis has deterministic features. Translational error was successfully employed as a tool to characterize the combustion dynamics before lean blowout in a gas turbine model combustor [9]. This method, proposed by Wayland *et al.* (1993), is used to obtain a quantitative measure of determinism in a time series. It is based on the idea that the neighboring trajectories in the state space align in similar directions if the time series has deterministic features [38]. For a measured time series data of pressure fluctuations,  $p'(t)$ , the set of delayed vectors are given by,

$$P(t) = \{p'(t), p'(t + \tau), \dots, p'(t + (D - 1)\tau)\} \quad (2)$$

where  $P(t)$  is the phase space vector at any time instant  $t$  and the elements of this vector represent coordinates of the corresponding vector in the  $D$ - dimensional phase space. The elements of this delayed vector can as well be viewed as the state variables of the dynamical system under study.

Let  $P(t_i)$  be an arbitrary vector in the phase space and  $P(t_j)$  ( $j=1,2, \dots, N$ ) be  $N$  nearest neighbors of the chosen vector. Let  $P(t_j + T)$  represent the delayed vectors after  $T$  time steps. The time interval  $T$  was suitably chosen to be the optimal time delay as we observed maximum determinism in the phase space at this choice of  $T$ .

An approximate tangent vector at time  $t_j$  is given by  $v(t_j)$ ,

$$v(t_j) = P(t_j + T) - P(t_j) \quad (3)$$

$\langle v \rangle$  denotes the average of the tangent vectors  $v(t_j)$  for  $j=1,2, \dots, N$

$$\langle v \rangle = \frac{1}{N+1} \sum_{j=0}^N v(t_j) \quad (4)$$

The translational error,  $E_{trans}$ , can be defined as

$$E_{trans} = \frac{1}{N+1} \sum_{j=0}^N \frac{\|v(t_j) - \langle v \rangle\|^2}{\|\langle v \rangle\|^2} \quad (5)$$

The value of translation error is approximately 1.0 for uncorrelated noise and close to zero for a periodic signal. The estimated value of  $E_{trans}$  will be close to zero if the degree of determinism visible in a time series is high. However, deterministic features can be considered as significant when  $E_{trans}$  for a signal is less than 0.1 [39]. It must be noted that there can be cases where the temporal correlations in a signal can be mistaken for determinism by the algorithms adopted for the analysis [40]. Hence, a single test alone might not be sufficient to detect chaos in the real world experimental data [30]. Further, the use of multiple measures of nonlinearity could prove useful to detect contamination with white or colored noise in a signal. Harikrishnan *et al.* (2009) illustrated an approach to detect white and colored noise in a time series

through the combined use of correlation dimension and correlation entropy. The procedure to find correlation dimension and entropy follows the GP algorithm. The delayed vectors are constructed as an initial step to estimate the dimension. Then, the average number of points within a distance  $R$  from an arbitrary phase space vector,  $P(t_i)$ , is given by

$$r_i(R) = \lim_{n \rightarrow \infty} \frac{1}{N} \sum_{j=1, j \neq i}^N H(R - |P(t_i) - P(t_j)|) \quad (6)$$

where  $N$  is the total number of delayed vectors constructed and  $H$  is the Heaviside step function. The correlation function,  $C(R)$ , is obtained by averaging  $r_i(R)$  over  $M$  selected delayed vectors.

$$C(R) = \frac{1}{M} \sum_{i=1}^M r_i(R) \quad (7)$$

Finally, the correlation dimension,  $D_2$ , is defined as

$$D_2 = \lim_{R \rightarrow 0} \frac{d \log C(R)}{d \log(R)} \quad (8)$$

The limitations of using GP algorithm to analyze a noisy time series were detailed before. To account for this, a non-subjective method, as described in Harikrishnan *et al.* (2006) was adopted to fix the scaling region, in order to correctly estimate the correlation dimension [41].

Further, correlation entropy, when employed in combination with AAFT surrogate, can detect colored noise embedded in a time series. The estimation of correlation entropy follows the same procedure as that for correlation dimension. Correlation entropy,  $K_2$ , is defined as

$$K_2 \delta t = \lim_{R \rightarrow 0} \lim_{D \rightarrow \infty} \lim_{M \rightarrow \infty} (-\log C(R)/D) \quad (9)$$

where  $\delta t$  is the time step used to generate the time series if the set of governing equations are known. In an experimental situation,  $\delta t$  can be chosen as the sampling time. A linear part in the  $\log C(R)$  vs  $\log(R)$  plot must be identified to estimate the correlation entropy [42]. This scaling region is computed algorithmically as described in Harikrishnan *et al.* (2008). Another suitable statistic that serves the purpose of this study is permutation entropy, which measures the degree of randomness observed in a time series. This measure relies on features that are based on ordinal pattern statistics. In this symbolic approach, a time series is partitioned into subsets of length  $D$  (embedding dimension), with its elements being separated by a delay  $\tau$ . Partitioning the time series in this manner is basically the same as phase space reconstruction. The possible permutations ( $D!$  permutations) for a sequence of length  $D$  are indexed as  $i$ , following a standard procedure [43]. The  $D!$  permutations are the possible ordinal patterns associated with this set of length  $D$ . Consider a sequence of length  $D$ , say

$\{p'(t), p'(t + \tau), p'(t + 2\tau), \dots, p'(t + (D - 1)\tau)\}$  obtained by partitioning the time series (non-consecutive points). The relative values of the elements are compared to find the order in which the elements appear in the set. The elements are then replaced by their ranks such that the elements with the smallest and largest value are assigned the rank '1' and 'D' respectively. This definite arrangement of elements can be assigned an index, called as the ordinal pattern index, following the procedure detailed in Parlitz *et al.* (2012). More details about ordinal patterns and the possible patterns associated with  $D = 4$  and 5 can also be found in Parlitz *et al.* (2012). Permutation entropy,  $h_p$ , is defined as

$$h_p = -\frac{\sum_{i=1}^{D!} p_i \log_2 p_i}{\log_2 D!} \quad (10)$$

Here,  $p_i$  represents the relative frequency of the ordinal pattern that is indexed as  $i$ . The estimates of  $h_p$  are then tested for their statistical significance using the RP, FT and AAFT surrogates.

Symbolic visual test is another simple and robust technique that can recognize regular, chaotic, stochastic and hyper-chaotic dynamics [44]. The permutation spectrum test (PST), as it is commonly called, is rather an extension of the Bandt and Pompe scheme [45] used to estimate the permutation entropy. Ordinal patterns of length  $D = 4$ , i.e., 24 possible patterns, are typically used, as it is computationally easier. The relative frequency of each ordinal pattern is used to derive a spectrum of ordinal patterns. The patterns are indexed according to the same convention as mentioned before. The relative frequency of certain patterns will be really high for a time series displaying regular dynamics. Thus, the specific patterns observed in the permutation spectra can be an indication of the nature of the time series under analysis. The presence of a large number of certain patterns in the time series indicates that there are many vectors pointing in similar direction in the reconstructed state space. Further, the ordinal patterns that are absent in the spectrum are termed as forbidden ordinal patterns. The presence of consistent forbidden ordinal patterns in the spectrum is an evidence of deterministic dynamics. A time series that displays regular dynamics, for instance, a periodic signal, will have only certain patterns in the permutation spectrum. It means that the spectrum for a periodic time series often contains only a small subset of the possible ordinal patterns. The remaining patterns will be absent in the spectrum. The same case applies to the permutation spectrum of any deterministic signal. A few forbidden patterns observed in the spectrum is an indication of the complexity of the time series [43]. The presence of few forbidden patterns in the spectrum means that a large subset of the possible ordinal patterns are visible in the time series. The presence of large subset of ordinal patterns observed in the time series is an indication of the complexity of the time series. Higher complexity also means a higher value of the permutation entropy for the signal. Forbidden patterns will be

absent if the analyzed time series is purely random [44]. In a random signal, there is no preference for any particular pattern. Thus, the probability of observing each of the possible ordinal patterns (corresponding to a particular  $D$ ) in the time series is the same. Therefore, no forbidden patterns can be observed in the permutation spectrum for a random signal. Further, PST is highly sensitive to the presence of noise in the time series. The forbidden patterns might disappear if the time series is contaminated with even small amount of noise. Ordinal patterns of larger permutation length, say  $D = 5$ , should be used to make sure that consistent forbidden patterns are observed [44].

In summary, the deterministic or stochastic nature of combustion noise has not been characterized accurately in the literature. A conclusive approach must be undertaken to ascertain the dynamic nature of combustion noise as its relevance extends to studies on critical transition to combustion instability. Fractal features in the pressure measurements acquired during the state of combustion noise are captured using the multifractal spectrum. In this study, we employ surrogate tests, with translational error and permutation entropy as the discriminating statistics, to test for determinism visible in the measured signal. In addition to this, permutation spectrum test is used to characterize the dynamic nature of the time series acquired from experiments. The nature of noise contamination in the signal could be qualitatively identified using correlation dimension and correlation entropy.

## II. EXPERIMENTAL SETUP

The unsteady pressure data was acquired from a swirl-stabilized as well as from a bluff-body stabilized backward facing step combustor. The schematics of the setup can be found in Nair & Sujith (2014). The main components of the setup are a settling chamber, a combustion chamber and a burner provided with a shaft to hold the bluff-body or swirler. The length of combustion chamber along with the extension ducts is around 700 mm. The bluff-body was located at a distance 50 mm from the backward facing step. A piezoelectric transducer (sensitivity  $72.5 \text{ mV kPa}^{-1}$ ,  $0.48 \text{ Pa}$  resolution,  $\pm 0.64 \%$  uncertainty) located 90 mm from the backward facing step was used to acquire the pressure measurements,  $p'(t)$ . A 16-bit AD conversion card (NI-643,  $\pm 5 \text{ V}$  input voltage range,  $\pm 0.15 \text{ mV}$  resolution) was used to acquire the voltage signal from the pressure transducer. The time series  $p'(t)$  (of 3 seconds duration) was acquired at a sampling frequency of 10 kHz. The ambient temperature was measured to be  $27 \pm 1 \text{ }^\circ\text{C}$  using a dry bulb thermometer and the relative humidity was measured to be  $85 \pm 1 \%$  on a hygrometer, when the pressure measurements were acquired [8, 10, 11].

### III. RESULTS

The time series of unsteady pressure  $p'(t)$  acquired from bluff-body stabilized (figure 1a) and swirl-stabilized combustor (figure 1c) during stable combustion are shown in figure 1. The pressure signal from bluff-body stabilized combustor has a Hurst exponent ( $H$ ) of  $0.20 \pm 0.002$  and a multifractal spectrum width of 0.65 as evident from figure 1b. The unsteady pressure data from the swirl-stabilized configuration has a Hurst exponent ( $H$ ) of  $0.15 \pm 0.002$  and a multifractal spectrum width of 0.68 as evident from figure 1d. The method of multifractal detrended fluctuation analysis (MFDFA) is used to obtain the multifractal spectrum [46].

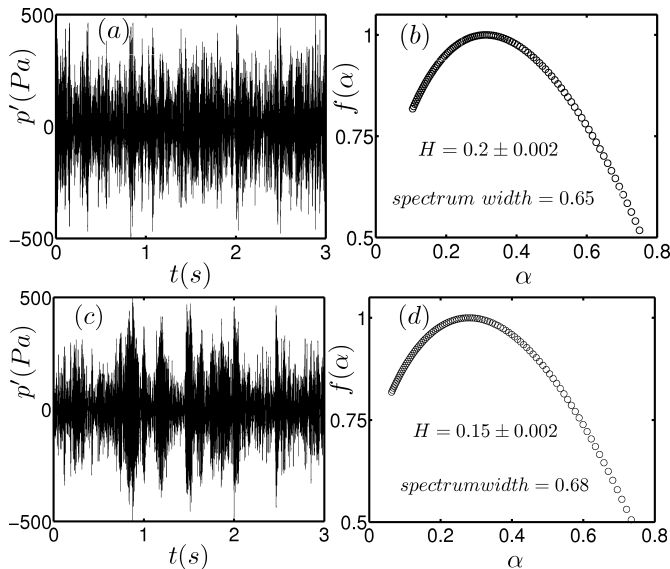


FIG. 1: Plot showing (a) the pressure time series acquired from (a) bluff-body and (c) swirl configurations and the singularity spectrum,  $f(\alpha)$ , as a function of the singularity strength,  $\alpha$ , for the experimental data sets. The multifractal spectrum presented in (b) and (d) correspond to the pressure data in (a) and (c) respectively. The values of Hurst exponent being less than 0.5 (for both (a) and (c)) illustrate the fractal nature of the observational time series data. The multifractal signature in the signal is illustrated through the finite width of the singularity spectrum. The above estimates for Hurst exponent and multifractal spectrum width are obtained from the pressure data of length,  $N = 30000$  data points, sampled at 10000 Hz, acquired from a turbulent combustor with bluff-body and swirl configurations.

It is known that Hurst exponent [47] is a measure that detects temporal correlations in a time series. It is a measure of self-similarity as it characterizes a fractal or multifractal time series with a scaling exponent or multiple scaling exponents respectively. The scaling of standard deviation for segments of different length or scale, obtained from the time series, is basically estimated as

Hurst exponent ( $H$ ) here. In other words, the corresponding scaling order  $q$  associated with the Hurst exponent discussed here is 2. Negative and positive orders ( $q$ ) can be adopted to detect small and large scale amplitude fluctuations in the time series. The Hurst exponents,  $H^q$ , estimated with these different scaling orders ( $q$ ), will be different if the time series has multifractal features. The finite width of the multifractal spectrum basically conveys the same information. It is clear that the time series obtained from experiments (swirl and bluff-body configurations) has a Hurst exponent that is less than 0.5. Therefore, the experimental data under study is an anti-persistent signal that displays multifractal features, as illustrated in figure 1. These temporal correlations observed in the experimental time series could arise from deterministic processes or the time series might as well be a correlated noise [26]. Hence, fractal features alone are not sufficient to conclude about the deterministic nature of the data under analysis.

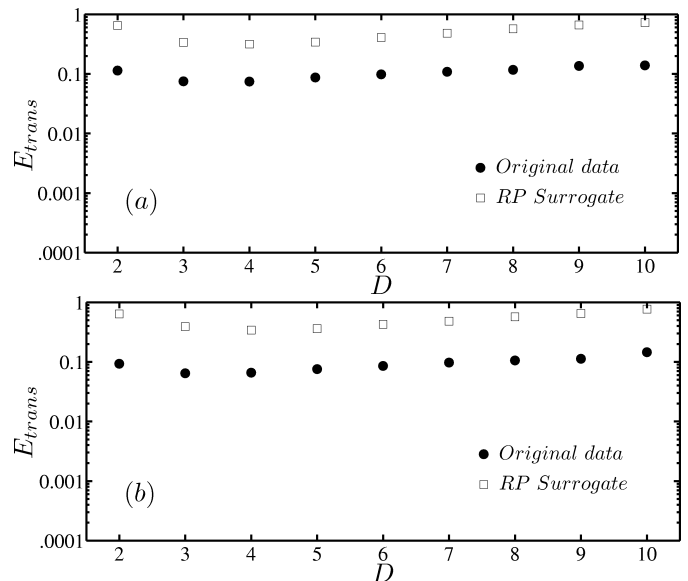


FIG. 2: Variation of translational error,  $E_{trans}$ , as a function of embedding dimension,  $D$ , for the pressure time series from (a) bluff-body and (b) swirl configurations and for the randomly shuffled surrogate data set. The estimates of translational error for the original data and the RP surrogates show a clear distinction between the two data sets. The significance level corresponding to RP surrogate is obtained to be 23.8 and 31.3 for the pressure data from bluff-body and swirl configuration respectively.

It is clear from the estimates of Hurst exponent and multifractal spectrum that the pressure time series acquired during the state of combustion noise possess fractal features. Tests for nonlinearity, along with surrogate methods, though on a statistical basis, could prove useful to recognize the dynamic nature of the time series. An ensemble of 19 surrogate data sets of the same length as the original time series is created so that the null hy-

pothesis can be rejected at 95 % confidence level, if the significance level  $t$  [Eq. (1)] is greater than 1.6. Translational error is used as a discriminating statistic for the analysis. Figure 2 shows the translational error for the experimental data from the two flame holding configurations as well as for the randomly shuffled surrogate data. It should be noted that the value of translational error must be less than 0.1 to characterize a time series as deterministic [6, 39]. The estimate of translational error for the experimental data is close to 0.1, making it difficult to conclude that it is deterministic. The sensitivity of the dynamical system to external noise is an important factor in this context. We find that, a dynamical system might be highly sensitive to noise such that the estimates of translational error might be much higher than 0.1 even for small amount of noise and vice versa. Therefore, there exists a possibility that the estimates of translational error obtained for the time series could be realized even with small amount of noise in the system.

Further, translational error is highly sensitive to the length of the time series for which the measure is calculated. The value of translational error for the shuffled surrogate is much less than 1, even though it is generated according to the null hypothesis of an uncorrelated random process. In case of white noise, a short time series must be examined, for the measure to give the expected value of 1. However, it is necessary to maintain the same length for the surrogate data sets as the original data to perform the surrogate test. Thus, the time series length  $N = 30000$  was maintained for the experimental data and for the ensemble of surrogate data sets generated from the experimental data. Further, the value of translational error at embedding dimension,  $D = 4$  is used as a representative value to compute the  $t$  value, as the measure attains a minimum almost at  $D = 4$ . The translational error for the experimental data is significantly lower than the RP surrogate. Rejection of the null hypothesis governing the RP surrogate means that the experimental data possess temporal correlations. This conclusion is consistent with the value of Hurst exponent estimated for the time series acquired from experiments. This motivates us to test the time series obtained from experiments, against the null hypothesis of FT and AAFT surrogates, to reach a conclusion about the dynamical nature of the time series.

Figure 3 shows the translational error for the experimental data from bluff-body and swirl configurations, as well as for the FT and AAFT surrogate data sets. In both cases (a and b), the estimates of translational error for the FT and AAFT surrogates appear closer to that of the experimental data. Thus, the null hypothesis of FT and AAFT cannot be rejected on a statistical basis at 95 % confidence interval, as evident from the corresponding  $t$  values. It must be noted that the  $t$  values corresponding to FT and AAFT surrogate data sets are much less than that of the RP surrogates. The limitations that can arise while developing the AAFT surrogates must be addressed here. The power spectrum of

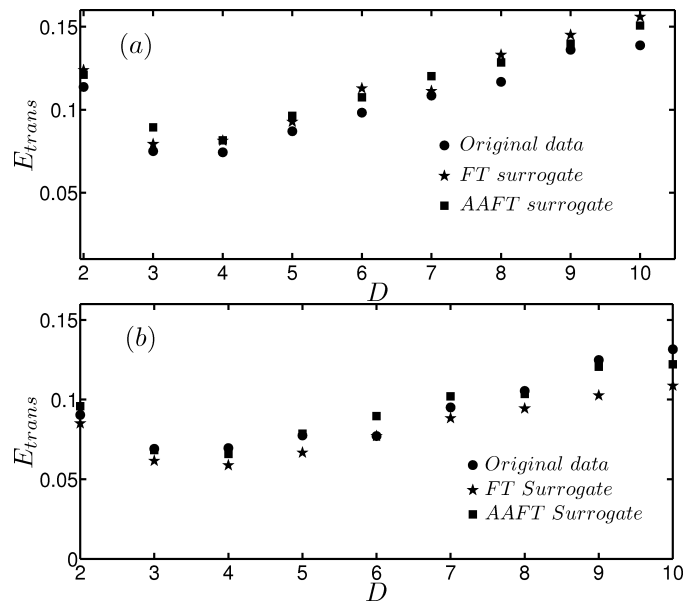


FIG. 3: Variation of translational error,  $E_{trans}$ , as a function of embedding dimension,  $D$ , for the unsteady pressure signal from (a) bluff-body and (b) swirl configuration, FT and AAFT surrogate data sets. The estimates of translational error for FT and AAFT surrogates appear close to that of the original data. The statistical significance of their difference can be evaluated at a certain confidence level. The significance level for the FT and AAFT surrogates are 1.33 and 1.04 respectively for the pressure data from bluff-body configuration while the significance level for the FT and AAFT surrogates are 1.44 and 0.49 respectively for the pressure data from swirl configuration.

the surrogate data may not be exactly the same as that of the original data after the rescaling process associated with the AAFT surrogate. The power spectrum can get slightly flattened under this procedure. Iterative algorithms must be used in order to correct such deviations in the periodogram [33, 34]. Taking into account of the limitations posed by AAFT, iterated AAFT was used to confirm the conclusion derived from AAFT. However, similar observation could be made if iterated AAFT is used instead of AAFT. Therefore, the results for iterated AAFT surrogate is not included in figure 3. Thus, the presence of nonlinearity in the time series corresponding to combustion noise obtained from experiments from swirl and bluff-body configurations could not be proven through surrogate analysis, with translational error as the discriminating statistic.

We proceed the surrogate analysis with a different discriminating statistic, the permutation entropy. Figure 4 shows the plot of normalized permutation entropy as a function of permutation order for the time series acquired from the two combustor configurations, as well as for shuffle, FT and AAFT surrogate data sets. It is computationally expensive to estimate this measure for

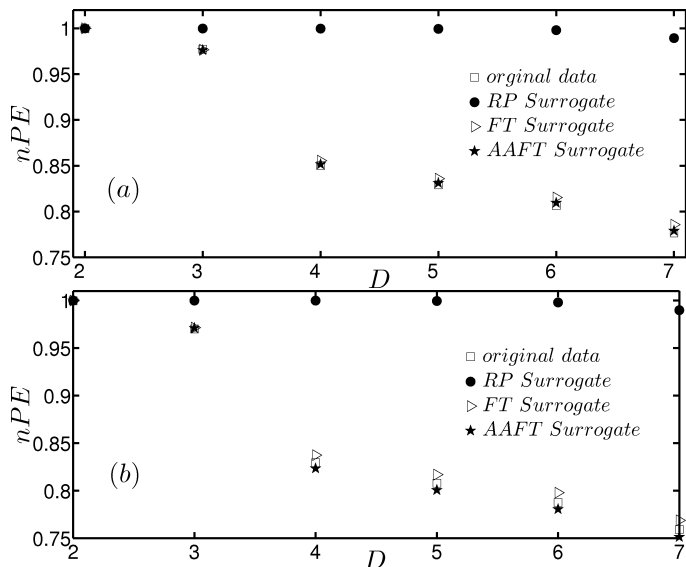


FIG. 4: Plot showing normalized permutation entropy,  $nPE$ , as a function of permutation order,  $D$ , for the acquired time series from (a) bluff-body and (b) swirl configurations, as well as for shuffled, FT and AAFT surrogate data sets. The estimate of permutation entropy for the original data is clearly different from that of the randomly shuffled surrogate data set. The estimates for the FT and AAFT surrogate data sets are not significantly different from that of the experimental series, as evident from the figure.

higher permutation orders i.e., for higher embedding dimension. Hence, the maximum permutation order was set to be seven. However, this statistic could not differentiate the original data from FT and AAFT surrogates as evident from the figure.

The presence of determinism in the time series is not evident from the surrogate tests performed, when translational error and permutation entropy are used as the discriminating measures. To further analyze the experimental time series, the symbolic visual test detailed before, called the permutation spectrum test, is adopted [44]. The Bandt and Pompe scheme [45] is used to implement the test and hence the name, permutation test. Figure 5 compares the spectrum of the experimental data from bluff-body (5a) and swirl (5b) configurations with that of high-dimensional chaotic data set (Mackey Glass system, figure 5c). The frequency of the ordinal patterns are estimated with  $D = 4$  and embedding delay=1 (consecutive points) as the parameters. 24 possible ordinal patterns are considered for this particular choice of  $D$ . The patterns in the spectra corresponding to the experimental and Mackey Glass data sets look similar. The ordinal patterns that do not appear in the time series data are called forbidden ordinal patterns. The frequency of these forbidden patterns will be zero in the permutation spectrum. Consistent forbidden patterns in the spectra for Mackey Glass data set confirm the deterministic na-

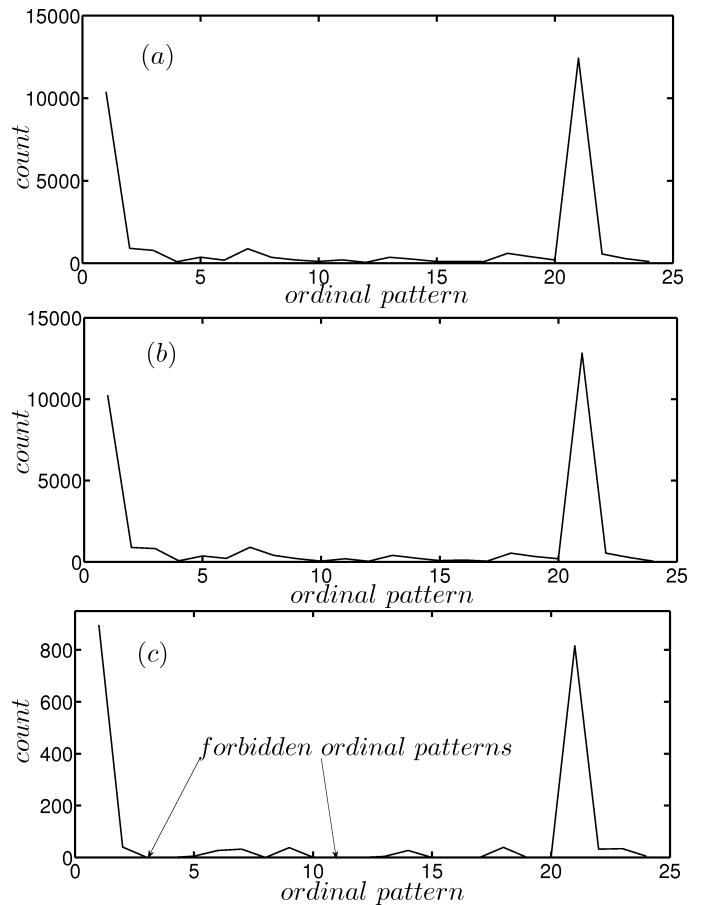


FIG. 5: Permutation spectra with  $D = 4$  and time lag ( $\tau$ ) = 1 for the pressure data acquired from (a) bluff-body and (b) swirl configurations (each of length  $N = 30000$  data points), (c) Mackey Glass chaotic time series of length  $N = 2000$  data points. The patterns for the two data sets (experimental and Mackey Glass chaotic data set) look similar. The presence of consistent forbidden ordinal patterns in the spectra for Mackey Glass chaotic data set indicates the deterministic nature of the time series. Such patterns are missing in case of the experimental data set, indicating the presence of noise in the time series.

ture of the time series. However, there are no forbidden ordinal patterns in the spectra of the experimental data in contrast to that of the Mackey Glass system. Therefore, no deterministic features could be observed in the spectra for the experimental data. The time series obtained from experiments can be contaminated with noise. There exists a possibility that the frequency of any of the patterns might be non-zero in the presence of a small amount of dynamic noise. There are some patterns that are dominant (higher frequency) in the pressure data as evident from figure 5a and 5b. In other words, it means that there are large number of vectors pointing in similar direction in the reconstructed phase space. This indicates that the data possesses temporal correlations. If

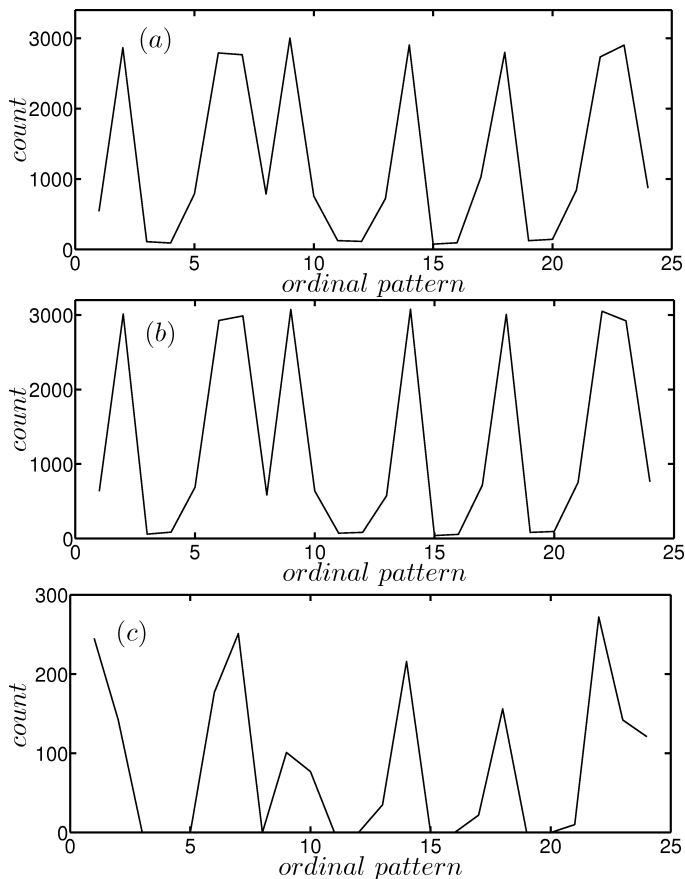


FIG. 6: Permutation spectra with  $D = 4$  and time lag ( $\tau$ ) = 11 for experimental data from (a) bluff-body and (b) swirl configurations (each of length  $N = 30000$  data points), (c) Mackey Glass chaotic time series of length  $N = 2000$  data points.  $\tau = 11$  is the embedding delay for both the data sets as obtained from the average mutual information. Notice the consistent forbidden patterns in the Mackey Glass chaotic data, which is a signature of determinism in the time series.

the data is purely random, the reconstructed vectors will be aligned in all directions and not in any specific direction. Therefore, a distinct peak may not be observed in the permutation spectrum of a completely random signal.

Consecutive elements in the time series form the members of the permutation sequence when a time delay of  $\tau = 1$  (as a multiple of sampling time) is chosen. The patterns in the spectrum, derived using consecutive elements in the time series, as shown in figure 5, might not be representing the actual system dynamics if the time series is contaminated with noise. This is because, the patterns in the spectrum for  $\tau = 1$  could as well be due to the noisy correlations in the data. The choice of delay is critical in such situations. Hence, a characteristic time scale must be an appropriate choice for  $\tau$ , while analyzing a noisy time series. The optimum time delay used for phase space reconstruction is an appropriate value for  $\tau$ . The average mutual information can

be used to estimate the optimum time delay. The average mutual information reaches its first minimum at  $\tau = 11$  for the pressure time series and it would be a proper choice for  $\tau$ . For this  $\tau$ , subsequences of the form  $\{p'(t), p'(t+\tau), p'(t+2\tau), \dots, p'(t+(D-1)\tau)\}$  are extracted from the time series, where  $t$  is a particular time instant. The permutation spectrum thus obtained through this partition will be much more reasonable and informative as far as the objective of this analysis is concerned. The patterns in the spectrum could thereby reveal the intrinsic dynamics of the system from the analyzed time series.

Figure 6 compares the PST of the experimental data from bluff-body (6a) and swirl (6b) configurations with that of high-dimensional chaotic data set (Mackey Glass system, figure 6c) estimated with  $D = 4$  and  $\tau = 11$  (non-consecutive points). Though the patterns look similar, the spectrum corresponding to the experimental data set does not possess any forbidden ordinal patterns, indicative of the presence of noise in the signal. Low values of frequency for certain ordinal patterns observed in the permutation spectra is suggestive of the potential forbidden ordinal patterns if the experimental data were not contaminated with noise. However, the similarity in the patterns observed in the spectra (between unsteady pressure data and Mackey Glass chaotic data) at time delays 1 and 11 might be a consequence of high dimensional chaos manifested in the experimental time series data.

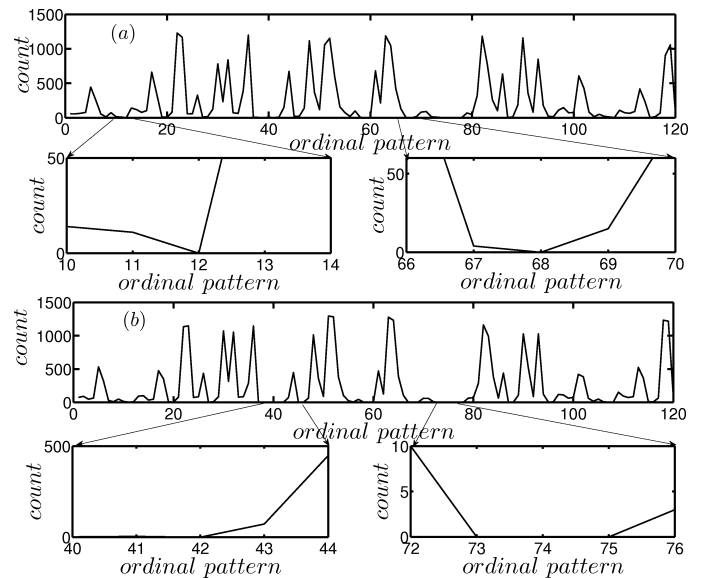


FIG. 7: Permutation spectra with  $D = 5$  and time lag ( $\tau$ ) = 11 for the experimental data from (a) bluff-body and (b) swirl configurations (each of length  $N = 30000$  data points). Notice the presence of certain forbidden ordinal patterns in the spectrum for pressure data from both configurations (see zoomed in view).

Certain forbidden patterns appeared for the PST with  $D = 5$  and  $\tau = 11$ , when it was implemented for the pressure time series acquired from bluff-body (7a) and swirl (7b) configurations (consisting of  $N = 30000$  data

points each), as shown in figure 7. This observation is similar to the result obtained for the noise driven sine map, as illustrated in Kulp & Zunino (2014).

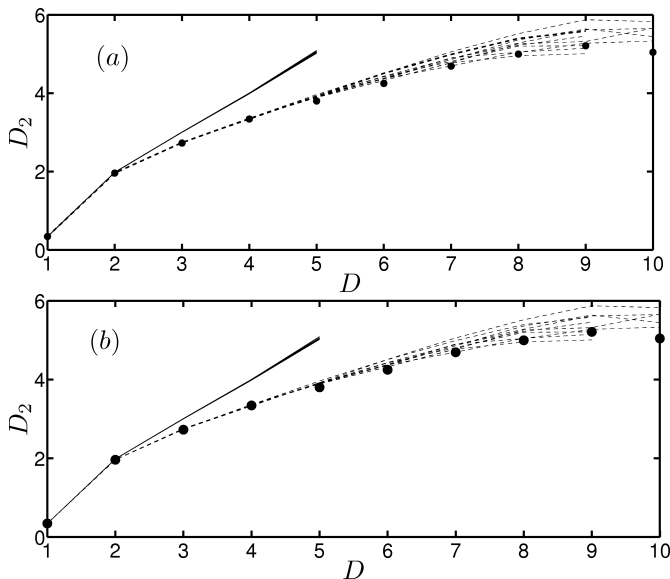


FIG. 8:  $D_2$  as a function of the embedding dimension ( $D$ ) for the experimental data ( $\bullet$ ) from (a) bluff-body and (b) swirl configurations, random shuffled surrogates ( $-$ ) and AAFIT surrogates ( $-$ ).  $D_2^{sat}$  is attained at  $D \sim 9 - 10$ , indicating the high dimensional nature of the system. An ensemble of 10 surrogates (random permutation and AAFIT surrogates) is used to obtain the plot. For the shuffled surrogate, the estimates of  $D_2$  is cut off at  $D = 5$ , as the trend of the curve clearly showed no saturation in  $D_2$ . The estimates of  $D_2$  for the experimental data sets (both a and b) closely resemble that of the ensemble of AAFIT surrogates. This observation for the experimental data is indicative of contamination with white noise.

To ascertain the claim that the data indeed has a deterministic nonlinearity of high dimensional nature, correlation dimension and correlation entropy are adopted. There is an additional objective underlying the choice of these measures. It is clear from the permutation spectrum that deterministic features are not discernable due to the presence of noise in the time series. The next task is to find the nature of this noise. It has been shown that the correlation dimension and entropy can possibly detect white and colored noise contamination in a signal [30]. The  $D_2$  estimates for the pressure data from both configurations, along with the corresponding shuffle and AAFIT surrogates, can be found in figure 8. The number of surrogates used for this analysis was limited to 10, for random and AAFIT surrogates. This is because the objective is not limited to assess the confidence level associated with the estimates for correlation dimension. Rather, the interest here extends to detecting the features of noise being embedded in the time series. It can be seen that,  $D_2$  does not attain a saturated value for

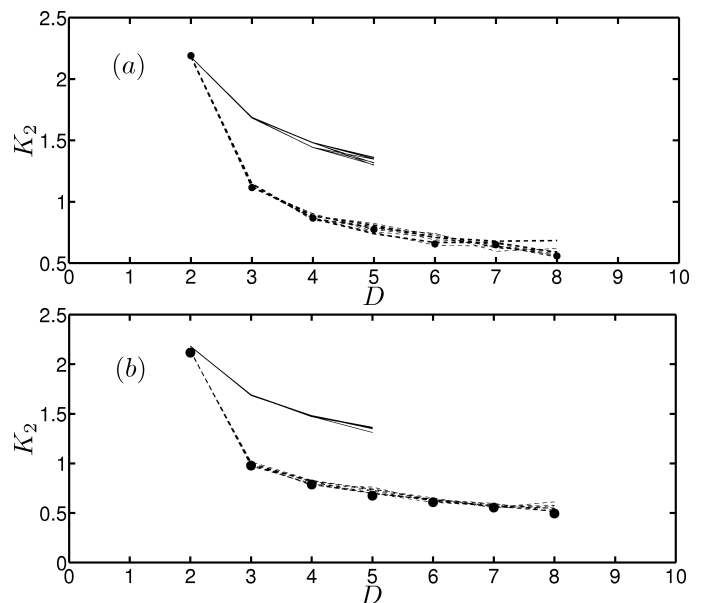


FIG. 9: Correlation entropy,  $K_2$  vs  $D$  for the experimental data ( $\bullet$ ) from (a) bluff-body and (b) swirl configurations, random shuffled surrogates ( $-$ ) and AAFIT surrogates ( $-$ ). An ensemble of 10 surrogates is used to compare the entropy estimates with that of the measured signal. The estimates of  $K_2$  for the experimental data sets (both a and b) do not significantly differ from the AAFIT surrogates indicating the presence of colored noise in the signal.

the ensemble of random surrogates. It is, therefore, consistent with the fact that a pure random signal must be infinite dimensional. Further,  $D_2^{sat}$  for the experimental data is observed at high embedding dimensions. Hence, it supports the conclusion that the measured signal has a high dimensional nature. Another significant observation is that original data and AAFIT surrogates have similar estimates for the correlation dimension. Earlier studies indicate that this observation might be an outcome of contamination with white noise in the signal [30]. This conclusion might not be valid without using a higher embedding dimension to obtain the estimate for correlation dimension. The estimates for correlation dimension could turn out to be inaccurate if the number of delayed vectors are insufficient or in other words, if the time series is short in length. This is because the number of reconstructed vectors depends on the embedding parameters used, and more importantly, this number decreases as the embedding dimension is increased. However, these factors do not undermine the following conclusions being derived from the analysis i.e.,  $D_2$  saturates at an embedding dimension close to 10 suggesting high dimensional dynamics and similar estimates for data and AAFIT surrogates indicating possible contamination with white noise. The presence of white noise might be a contribution from the measurement system as observational noise is expected to be unrelated to the system dynamics.

Further, the presence of dynamic noise in the signal is also expected. It is often difficult to detect noise of this nature as it possesses temporal correlations. This difficulty persists, irrespective of the nature of the system; i.e., low or high dimensional system, from which the time series is acquired. The estimates of correlation entropy for the original data can be compared to that of the AAFT surrogates to establish the presence of correlated noise in the time series. Figure 9 illustrates the correlation entropy as a function of embedding dimension for the experimental data, random shuffled and AAFT surrogate sets. The estimates of correlation entropy for AAFT surrogate data sets follow that of the original data as evident from figure 9. It is also clear from the permutation spectrum that the experimental data has features of high dimensional chaotic signal (see figures 5 and 6). Hence, we conclude that the data is generated from a deterministic process and not an outcome of a stochastic process. Thus, the estimates of AAFT surrogates being similar to that of the experimental data suggests possible contamination with colored noise [30].

In summary, we conclude that the pressure fluctuations during the state of combustion noise has the features of high dimensional chaotic data. We show that the pressure data is contaminated with white and colored noise. We find that the pressure data from swirl-stabilized combustor has similar dynamical features as that of the data from a bluff-body stabilized combustor. This observation indicates that the features of combustion noise are independent of the flame holding configuration of the combustor. Earlier studies [8, 11] have shown that combustion noise is multifractal and that the pressure fluctuations have dynamical features which resemble that of a chaotic signal. Nair *et al.* (2013) adopted local flow test (Kaplan Glass test) along with Random Permutation test to identify if these aperiodic pressure fluctuations have a deterministic signature. Kaplan Glass method is similar to translational error as both measures are based on the idea that the trajectories of a deterministic signal will have similar direction in a given region in the reconstructed phase space. The estimates of Kaplan Glass method and translational error provides the degree of determinism in the phase space. However, appropriate surrogate methods must be adopted to completely distinguish the time series from a stochastic signal if Kaplan Glass method is used as a test for determinism. The estimates of the pressure data for any statistic, being different from that of the RP surrogate, do not provide any conclusive proof that the original data is deterministic. This observation merely indicates that the pressure data possesses temporal correlations. Therefore, it is necessary to adopt FT and AAFT surrogates in addition to the RP surrogates to conclusively prove that the data is deterministic in nature. Further, Nair *et al.* (2013) used 0–1 test for chaos to determine the dynamic nature of pressure fluctuations. However, 0–1 test, by itself, cannot distinguish a chaotic

signal from a correlated stochastic process [48, 49]. In short, Nair *et al.* (2013) used two measures along with RP surrogate to conclude that the pressure data is chaotic in nature. Therefore, the analysis carried out by Nair *et al.* (2013) is not conclusive. In this study, we employed additional surrogate methods such as FT and AAFT surrogates to check if the original data is indeed deterministic or merely an outcome of a stochastic process. We used multiple measures to test for determinism visible in the pressure measurements. To avoid false rejections, we calculated the significance level for the estimates of different statistics based on the total number of surrogates used. We used correlation entropy and correlation dimension to find the nature of noise contamination in the pressure data.

#### IV. DISCUSSIONS

The combined use of measures, Hurst exponent, translational error, permutation entropy, permutation spectrum, correlation dimension and correlation entropy, reveal that the time series acquired during the state of combustion noise exhibits high dimensional chaotic dynamics. Further, the pressure data is contaminated with measurement (white) and dynamic (colored) noises, as evident from the estimates of correlation dimension and entropy. In the analysis, we find that the discriminating measures adopted are sensitive to noise. Thus, a single metric is not sufficient to conclude about the features of a time series acquired from experiments. It also turns out that the surrogate tests, employed in this study, could not reveal any nonlinearity present in the measured signal. This motivated us to adopt a symbolic visual test called permutation spectrum test to recognize the dynamic nature of the pressure data obtained from experiments. Further, the permutation spectrum adopted in this study could be used a tool to study different states observed in dynamical systems, such as intermittency, quasiperiodicity etc. In addition to this, the spectrum test is efficient to characterize the nature of a time series even if it is contaminated with noise.

#### ACKNOWLEDGEMENTS

This study was funded by ONR Global (Contract Monitor: Dr. R. Kolar). We thank Dr. V. Nair (KTH, Stockholm) for providing the experimental data used for this study and for the code to compute average mutual information and singularity spectrum. We acknowledge the discussions with Prof. G. Ambika (IISER, Pune). We also are grateful to Dr. H. Gotoda (Tokyo University of Science, Japan), for sharing the MATLAB code for translational error and Dr. K. P. Harikrishnan (The Cochin College, Cochin) for providing the code for correlation dimension and entropy.

- 
- [1] F. E. C. Culick. AGARD 72 B PEP Meeting, England, 7 Rue Ancelle 92200 Neuilly Sur Seine France, 1988.
- [2] K.R. McManus, T. Poinsot, and S.M. Candel. *Prog. Energy Combust. Sci.*, **19**:1, 1993.
- [3] T. C. Lieuwen. *Unsteady Combustor Physics*. Cambridge University Press, Cambridge, UK, 2012.
- [4] A. C. Altunlu, P. J. M. van der Hoogt, and A. de Boer. *J. Eng. Gas Turbines Power*, **136**:051501, 2014.
- [5] E. H. Perry and F. E. C. Culick. *Combust. Sci. Technol.*, **9**:49, 1974.
- [6] H. Gotoda, H. Nikimoto, T. Miyano, and S. Tachibana. *Chaos*, **21**:013124, 2011.
- [7] H. Gotoda, M. Amano, T. Miyano, T. Ikawa, K. Maki, and S. Tachibana. *Chaos*, **22**:043128, 2012.
- [8] V. Nair, G. Thampi, S. Karuppusamy, S. Gopalan, and R. I. Sujith. *Intl. J. Spray. Combust. Dyn.*, **5**:273, 2013.
- [9] H. Gotoda, Y. Shinoda, M. Kobayashi, Y. Okuno, and S. Tachibana. *Phys. Rev. E*, **89**:022910, 2014.
- [10] V. Nair, G. Thampi, and R. I. Sujith. *J. Fluid Mech.*, **756**:470, 2014.
- [11] V. Nair and R. I. Sujith. *J. Fluid Mech.*, **747**:635, 2014.
- [12] L. Kabiraj, A. Saurabh, N. Karimi, A. Sailor, E. Mastorakos, A. P. Dowling, and C. O. Paschereit. *Chaos*, **25**:023101, 2015.
- [13] Y. Okuno, M. Small, and H. Gotoda. *Chaos*, **25**:043107, 2015.
- [14] S. T. Trickey, L. N. Virgin, and E. H. Dowell. *Proc. Math. Phys. Eng. Sci.*, **458**:2203, 2002.
- [15] Z. Zhang and S. R. K. Nielsen. *Proc. of the 9th International Conference on Structural Dynamics, EURO-DYN*, page 3691, 2014.
- [16] V. Nair. *Role of intermittency in the onset of combustion instability*. Indian Institute of Technology, Madras, Chennai, Tamil Nadu, India, 2014.
- [17] B. Muhlbauer, R. Ewert, O. Kornow, B. Noll, J. Delfs, and M. Aigner, 2008.
- [18] N. Noiray and B. Schuermans. *Intl. J. Non-Linear Mech.*, **50**:152, 2013.
- [19] N. Noiray and B. Schuermans. *Proc. R. Soc. A*, **469**:20120535, 2013.
- [20] S. Lepri, G. Giacomelli, A. Politi, and F.T. Arecchi. *Physica D*, **70**:235, 1994.
- [21] L. Kabiraj, A. Saurabh, P. Wahi, and R. I. Sujith. *Chaos*, **22**:023129, 2012.
- [22] L. Kabiraj and R. I. Sujith. *J. Fluid Mech.*, **713**:376, 2012.
- [23] J. Theiler, S. Eubank, A. Longtin, B. Galdrikian, and J. D. Farmer. *Physica D*, **58**:77, 1992.
- [24] M. Murugesan and R. I. Sujith. *J. Fluid Mech.*, **772**:225, 2015.
- [25] K. Vibe and J. Vesin. In *Proc. 15eme Colloque sur le Traitement des Signaux et Images, Juan-les-Pins, France*, Signal processing of HDTV-IV, page 77. IEEE, 1995.
- [26] S. J. Schiff, T. Sauer, and T. Chang. *Integr. Physiol. Behav. Sci.*, **29**:246, 1994.
- [27] A. S. Pikovsky. *Phys. Lett. A*, **165**:33, 1992.
- [28] V. I. Oseledec. *Trans. Moscow Math. Soc.*, **19**:197, 1968.
- [29] A. Stefanski. *J. Theo. Appl. Mech.*, **46**:665, 2008.
- [30] K. P. Harikrishnan, R. Mishra, and G. Ambika. *Comm. in Nonlinear Sci. and Numerical Simulation*, **14**:3608, 2009.
- [31] J. P. Eckmann and D. Ruelle. *Physica D*, **56**:185, 1992.
- [32] T. Chang, T. Sauer, and S. J. Schiff. *Chaos*, **5**:118, 1995.
- [33] T. Schreiber and A. Schmitz. *Physica D*, **142**:346, 2000.
- [34] K. T. Dolan and M. L. Spano. *Phys. Rev. E*, **64**:046128, 2001.
- [35] C. Chatfield. *The analysis of time series: an introduction*. CRC Press, Florida, US, 6th edition, 2004.
- [36] J. Theiler and D. Prichard. *Physica D*, **94**:221, 1996.
- [37] V. Nair and R. I. Sujith. *Chaos*, **23**:033136, 2013.
- [38] R. Wayland, D. Bromley, D. Pickett, and A. Passamante. *Phys. Rev. Lett.*, **70**:580, 1993.
- [39] D. J. Wales. *Nature, London*, **350**:485, 1991.
- [40] J. Theiler. *Phys. Lett. A*, **155**:480, 1991.
- [41] K. P. Harikrishnan, R. Mishra, G. Ambika, and A.K. Kembhavi. *Physica D*, **215**:137, 2006.
- [42] K. P. Harikrishnan, R. Mishra, and G. Ambika. *Pramana J. Physics*, **72**:325, 2008.
- [43] U. Parlitz, S. Berg, S. Luther, A. Schirdewan, J. KurthS, and N. Wessel. *Comput. Bio. Med.*, **42**:319, 2012.
- [44] C. W. Kulp and L. Zunino. *Chaos*, **24**:033116, 2014.
- [45] C. Bandt and B. Pompe. *Phys. Rev. Lett.*, **88**:174102, 2002.
- [46] E. A. F. Ihlen. *Front. Physiol.*, **3**:141, 2012.
- [47] H. E. Hurst. *Trans. Amer. Soc. Civil Eng.*, **116**:770, 1951.
- [48] G. A. Gottwald and I. Melbourne. *SIAM J. Appl. Dyn. Sys.*, **8**:129, 2009.
- [49] J. Hu, W. Tung, J. Gao, and Y. Cao. *Phys. Rev. E*, **72**:056207, 2005.